Between two furrows: soil bulk density from non-invasive seismology

by Tsekhmistrenko, M., Collins, J., Bloem, H., Fallah, T., Ritsema, J., Jeffrey, S. and Nissen-Meyer, T.

Tsekhmistrenko, M., Collins, J., Bloem, H., Fallah, T., Ritsema, J., Jeffery, S. and Nissen-Meyer, T. (2025) 'Between two furrows: soil bulk density from non-invasive seismology', *Environmental Research Communications*, 7(11), article number 111010.

Environmental Research Communications

OPEN ACCESS

RECEIVED
27 May 2025

REVISED
23 August 2025

ACCEPTED FOR PUBLICATION
7 November 2025

PUBLISHED
25 November 2025

LETTER

Between two furrows: soil bulk density from non-invasive seismology

Maria Tsekhmistrenko[1,*], **Joe Collins**[1,2], **Hugo Bloem**[1], **Tina Fallah**[1,2], **Jeroen Ritsema**[3], **Simon Jeffery**[1,2] and **Tarje Nissen-Meyer**[1,4]

[1] Earth Rover Program, United Kingdom
[2] Harper Adams University, United Kingdom
[3] Department of Earth and Environmental Sciences, University of Michigan, United States of America
[4] Department of Mathematics & Statistics, University of Exeter, United Kingdom
[*] Author to whom any correspondence should be addressed.

E-mail: maria@earthroverprogram.com

Keywords: bulk density, imaging, instrumentation, soil, seismology

Supplementary material for this article is available online

Abstract

Soil is a critical resource for global food security. However, traditional physical analyses of soil samples and geophysical imaging techniques are often labour intensive and time-consuming. This study investigates the potential of ultra high-frequency (> 500 Hz) hammer-source seismology to characterise the physical properties of soil at the decimetre scale. We conducted experiments within a long-term field experiment near Harper Adams University (UK) aimed at comparing Conservation and Conventional agriculture. We surveyed two meter-and-a-half sections of each agricultural treatment with 16 geophones and collected soil samples with the same horizontal resolution. Our estimates of the P-wave velocity (v_p) and bulk density in the upper 40 cm of the soil reveal a strong and statistically significant correlation. Consistent correlation of bulk density and v_p throughout the depth profile were observed between the seismic images and interpolated bulk density data derived from physical soil samples. Our work demonstrates that ultra-high frequency seismic analysis is a promising, cost-effective tool for estimating soil bulk density, in support of agronomic and land-management decision making, and improving the accuracy of soil carbon stock quantification.

1. Introduction

Soil is the most important ecosystem for global food security. More than 99% of the calories humans consume are produced in soil (Pimentel 2006). Yet, research of the chemical, physical and biological structures of soil is limited, and incomplete global monitoring of soil hinders the progress in soil sciences and the improvement of agricultural practices. This is especially important as the combination of land degradation and climate change are predicted to reduce crop yields by an average of 10% globally, and up to 50% in certain at-risk regions by 2050, resulting in the forced migration of 50 to 700 million people (Scholes *et al* 2018).

Soil is a conglomeration of sand, silt, clay and organic materials. Biological activity, from microbes (Tisdall and Oades 1982, Neal *et al* 2020) to earthworms (Sharma *et al* 2017), shape soil into a porous matrix. The physical structure of soil is hierarchical from micro- to macro-aggregates (Dexter 1988, Basset *et al* 2023), which have direct and indirect effects on ecosystem function, agricultural productivity, and environmental sustainability through its interactions with plant growth and crop production, water infiltration and gas diffusion (Jarvis *et al* 2024). Macro-aggregates may form distinct structures, such as 'blocky' formations, 'columns' (common in soils with high sodium content), or 'massive' structures, typically resulting from compaction due to trafficking or repeated tillage. These structures can significantly decrease soil permeability to both gases and water. Soil genesis and maintenance therefore constitute a key part of soil health (Lehmann *et al* 2020).

Currently there exist no effective means of exploring soil structure at either a macro-aggregation or soil horizon scale (< 1 m) without digging a soil pit or taking undisturbed soil cores, as techniques such as x-ray tomography lack field-scale applicability, and geophysical techniques such as electrical resistivity and ground-penetrating radar provide spatial information but struggle to characterize key properties like bulk density and horizon depth (Jeffery *et al* in prep.). Location-specific sampling is expensive and labour intensive, so extrapolation to the field (100 m) or landscape scale (1–10 km) is inevitable. This severely impacts our understanding of soil health as key soil properties are known to be highly spatially and temporally variable (Usowicz and Lipiec 2017, Lehmann *et al* 2020, Nyéki *et al* 2022).

Bulk density is a key property for calculating soil organic carbon (SOC) stocks, quantifying compaction levels, top soil volume, and carbon concentration (Minasny *et al* 2013), and for modelling a wide range of soil processes (e.g. how carbon moves and is stored in the soil, or microbial activity and CO_2 fluxes) (dos Santos *et al* 2025). However, measuring the bulk density of soil is particularly difficult as it is labour intensive, time-consuming, and expensive (Suuster *et al* 2011). Therefore, rather than directly measured in the field, bulk density is usually estimated using a mathematical model known as a pedotransfer function (Hollis *et al* 2012, Suuster *et al* 2011), especially at the landscape or larger scale. For example, Liu *et al* (2013) use equations developed by Saxton *et al* (1986) to model SOC stocks in North America, based on the Unified North American Soil Map. To circumvent the logistical difficulty of measuring bulk density at scale, recent research has focused on machine-learning models to identify pedotransfer functions at the continental scale. For example, dos Santos *et al* (2025) uses a comprehensive dataset of soil properties in Brazil to present a machine learning model that accurately predicts bulk density, which outperformed a multiple linear regression approach. In addition, Chen *et al* (2024) uses the European 'Land Use/Cover Area frame statistical Survey Soil' databases (Orgiazzi *et al* 2018) to train a machine learning model using 15 predictor variables, which outperformed previous non-machine learning based pedotransfer functions.

Seismology provides a non-invasive method for studying Earth's mantle (Nolet 2008) and crust (Rawlinson *et al* 2010). However, it has rarely been considered a useful tool for investigating Earth's shallowest layer—the soil. The visibility of interfaces in seismic imaging strongly depends on velocity contrasts and layer definition; poorly defined interfaces cause scattering and ambiguous data, making it harder to interpret depth and layering. While previous studies have examined soil compaction or wave velocity at moderate resolutions (Lu *et al* 2019, Carrera *et al* 2024), we propose a seismic method using ultra-high frequencies to investigate soil bulk density in the soil 'A' Horizon.

Soil profiles are divided into layers, called horizons, which are usually parallel to the soil surface. The 'O' and 'A' horizons, commonly referred to as the 'topsoil' by farmers, are of particular importance in soil science and agriculture, as they store the majority of the soils biota, nutrients and organic matter (Hartemink *et al* 2020). Therefore, management tools which can accurately quantify the physical structure of the topsoil are beneficial to soil health and carbon sequestration in soils. Recent papers have highlighted how active source seismology can help overcome the logistical complexities of characterizing soils at small scales. For example, Lu *et al* (2019) and Carrera *et al* (2024) measured the frequency-dependent phase velocity of Rayleigh waves to characterise the depth profiles and horizontal variations of soil horizons with strong contrasts. Romero-Ruiz *et al* (2021) identified changes in phase velocity down the soil profile using seismology and was able to characterise changes in bulk density. Carrera *et al* (2024) also identified changes in phase velocity down the vertical soil profile and imposed specific depths (0–30 cm, 60–100 cm and >100 cm) to parametrise their model of the sub-soil.

In this study, we refer to frequencies below 50 Hz as low-frequency, 50–500 Hz as high-frequency, and frequencies above 500 Hz. This classification is based on two main factors; A: the typical operational range of seismic instruments, which generally falls below 200 Hz, and; B: the existing literature, where frequencies above 200 Hz are rarely explored. Further, the term 'ultra-high frequency' is deliberately chosen, as 'high-frequency' is commonly used in geophysics, often referring to ~1 Hz in global seismology and up to 100 Hz in exploration seismology.

In order to map soil physical structure at the decimetre scale, we need to use seismic waves with sufficiently small wavelengths to identify small changes in physical structure along their propagation path. For the topsoil case, this suggests using frequencies above 500 Hz. While previous seismic experiments have quantified changes to soil bulk density at lower depths (50–100 cm) (Carrera *et al* 2024), quantification of soil bulk density and the spatial variation within the soils 'A' horizon requires ultra-high frequencies. Typically, wave velocities are known to be affected by various soil properties including moisture (Baker *et al* 2002), temperature (Park and Kim 2023), lithology (El-Emam *et al* 2019). A systematic comparison of the seismic and physical properties of soil is an important step toward quantifying of SOC stocks.

This study is the first step in a longer-term effort to build a reference database that links seismic wave speeds and soil horizon depths to key soil properties, including soil type, structure, moisture content, bulk density, compaction, and their seasonal variability. Over time, and through repeated measurements across a range of

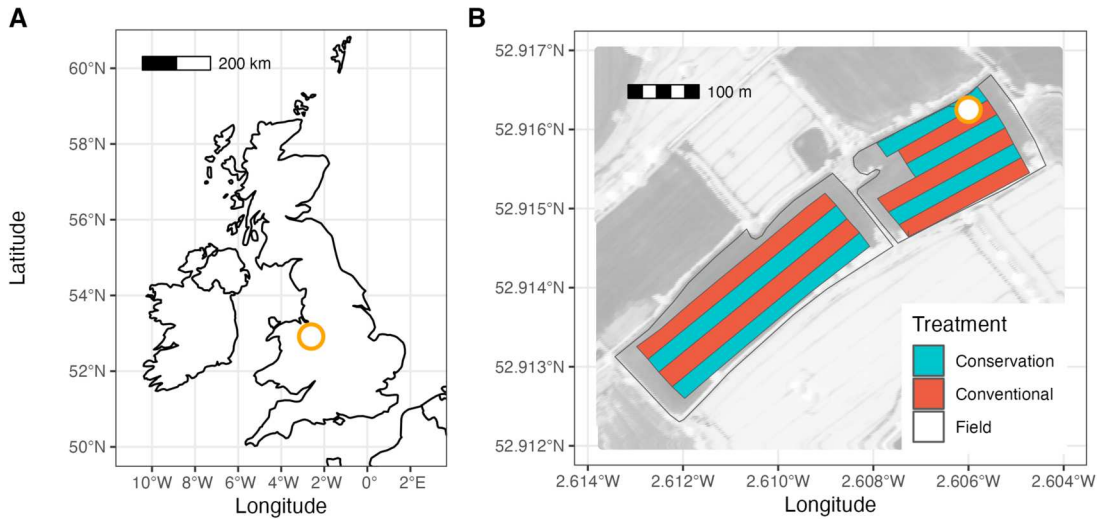

Figure 1. A Map of the experimental location in Shropshire, UK. The orange circle indicates the field site. **B** The design of the agricultural systems experiment. The Conventional treatment is denoted by the red shading and the Conservation treatment by the blue shading. The orange circle shows the exact location where the seismic experiment and soil sampling was conducted. Reproduced with permission from [Collins (2025)].

Table 1. Comparison of agricultural practices under Conventional and Conservation treatments in the field experiment.

Conventional agriculture	Conservation agriculture
Tillage used when deemed necessary	Minimal soil disturbance through direct drilling of all crops; no cultivation
Removal of straw residue	Maintenance of soil cover by chopping straw residue back onto the soil surface and use of direct drilling
No use of cover crops	Diversified crop rotation through the inclusion of cover crops
Insecticide usage	No use of insecticides

environments and conditions, the aim is to develop a tool that could eventually support land management and empower farmers to undertake non-invasive soil health monitoring at high resolution. Our use of ultra-high frequency, active small-scale source seismology is an intentionally simple, affordable, and scalable approach, designed to explore its feasibility as a practical method for soil monitoring.

2. Methods

2.1. Field site

The experiment was located in north Shropshire, UK (Lat 52.915, Lon −2.606). The site consists of an experiment involving two adjacent fields (figure 1), measuring 3.7 ha and 5.7 ha in area. The main soil type of the site is a sandy clay loam, which is classified by the National Soil Resources Institute as a slowly permeable seasonally wet slightly acid but base-rich loamy and clayey soils (Hallett *et al* 2017). The site is drained with 100 mm diameter clay piping at a depth of 1.2 m.

The experiment consists of a systems-level comparison of Conservation Agriculture and Conventional crop production systems with 10 plots and five replicates using a systematic plot design (Collins 2025). Plots were 24 m wide and varied in length according to field shape. All machinery operations were conducted by local agricultural contractors. The two systems were managed independently by qualified agronomists, one specialising in commercial agronomy and the other specialising in conservation (regenerative) agronomy. The crop management was performed by the agronomists independently for each system. The agronomic decisions were devised from regular field observations during the season, as is common practice in a commercial setting. The experimental treatments were managed using the principles summarised in table 1.

2.2. Hammer seismics

We conducted the experiments on January 31st and February 1st, 2025, during the fourth year of the agricultural experiment. Conventional treatment was planted with winter wheat (*Triticum aestivum* var.

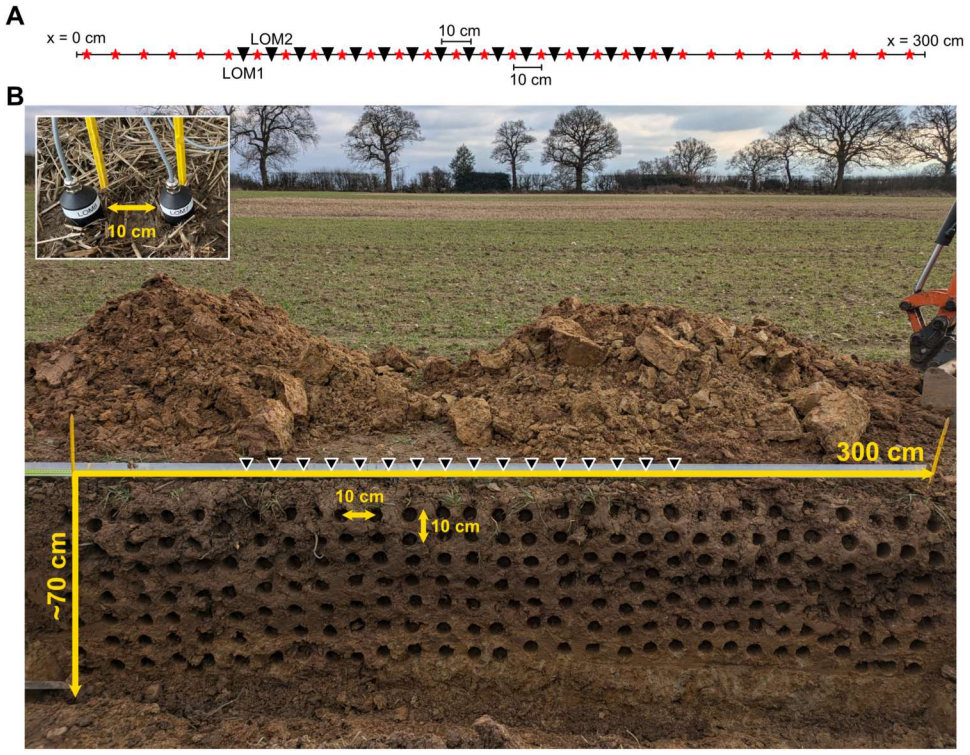

Figure 2. A Schematics of experimental set-up. In total 16 instruments were used (black inverted triangles). The red stars show the hammer strike location. **B** Photograph of the detailed soil sampling which was conducted right beneath the seismic experiments (black inverted triangles with white rim show approximate location of the geophones). Horizontal yellow line measures the extend of the trench (300 cm), vertical yellow line measures the depth of the trench. In total 210 soil samples were taken, with approximately 10 cm spacing between them, and analysed for each experimental treatment. Inlay shows zoom of LOM instruments during experiment.

Extase) on October 5th, 2024, and the Conservation treatment was left fallow over the winter months. The Conventional treatment was established by ploughing to a depth of 25 cm, the furrows worked with a power harrow, and winter wheat drilled to a depth of 4 cm. The seismic experiment was conducted 6 m from the plot edge and 6 m from the tramline centre within the northeastern quadrant of the field (figure 1(B)).

We used a hammer source to generate waves (240 g hammer striking a 5-cm square plate) and recorded the seismic waves with 16 LOM geophones. The LOM records ground motions and has sensitivity to frequencies between 10 and 2000 Hz (`https://store.lom.audio/`, Bloem *et al* (2025)). We placed the LOMs at a distance of 60 cm to 190 cm from $x = 0$ with a uniform spacing of 10 cm. Thirty hammer locations were performed starting at $x = 5$ to 295 cm at 10 cm increments (figure 2(A)). Figure 3 shows common receiver gathers (i.e., records of multiple hammer strikes at the same station) for both treatments. The geophones were located at $x = 60$ cm (LOM1) and $x = 70$ cm(LOM2) respectively.

We used 'Snuffler' from the `Pyrocko` software library (Heimann *et al* 2017) to pick P-wave arrival times. We varied the low-pass and high-pass filter setting between 500–1500 Hz and 1500–2000 Hz to maximize the signal-to-noise ratio in the vicinity of the P-wave onset. We obtained 458 and 496 travel-time data points for Conservation and Conventional treatments, respectively. We estimated the 2-D P-wave velocity (v_p) structure beneath the seismic lines using the `pyGIMLi` software (Rücker *et al* 2017), which is a ray-based approach using Dijkstra's algorithm for efficient first-arrival travel times calculations. The inversion was based on a Gauss-Newton scheme (Wang 2012) with Tikhonov regularization.

We quantified the v_p to a depth of 40 cm at triangular grid points. The mesh consisted of a triangular grid with average element sizes of 5 cm near the surface, increasing with depth to around 15 cm, to ensure accurate ray bending and turning. We used a smooth, linear, starting model based on default starting values of `pyGIMLi` (top: 500 m s^{-1}; bottom: 5000 m s^{-1}) and assumed constant uncertainties for the manual picks between 0.45 and 0.55 millisecond. We obtained the final model for v_p by minimizing the least-squares difference between calculated and measured P-wave arrival times. In seismic tomography, we refer to this resulting distribution as a 'model', which is a spatial dataset of seismic velocities derived from traveltime inversion, not a predictive or statistical model. The final 'seismic image' is a visual representation of this inferred velocity model.

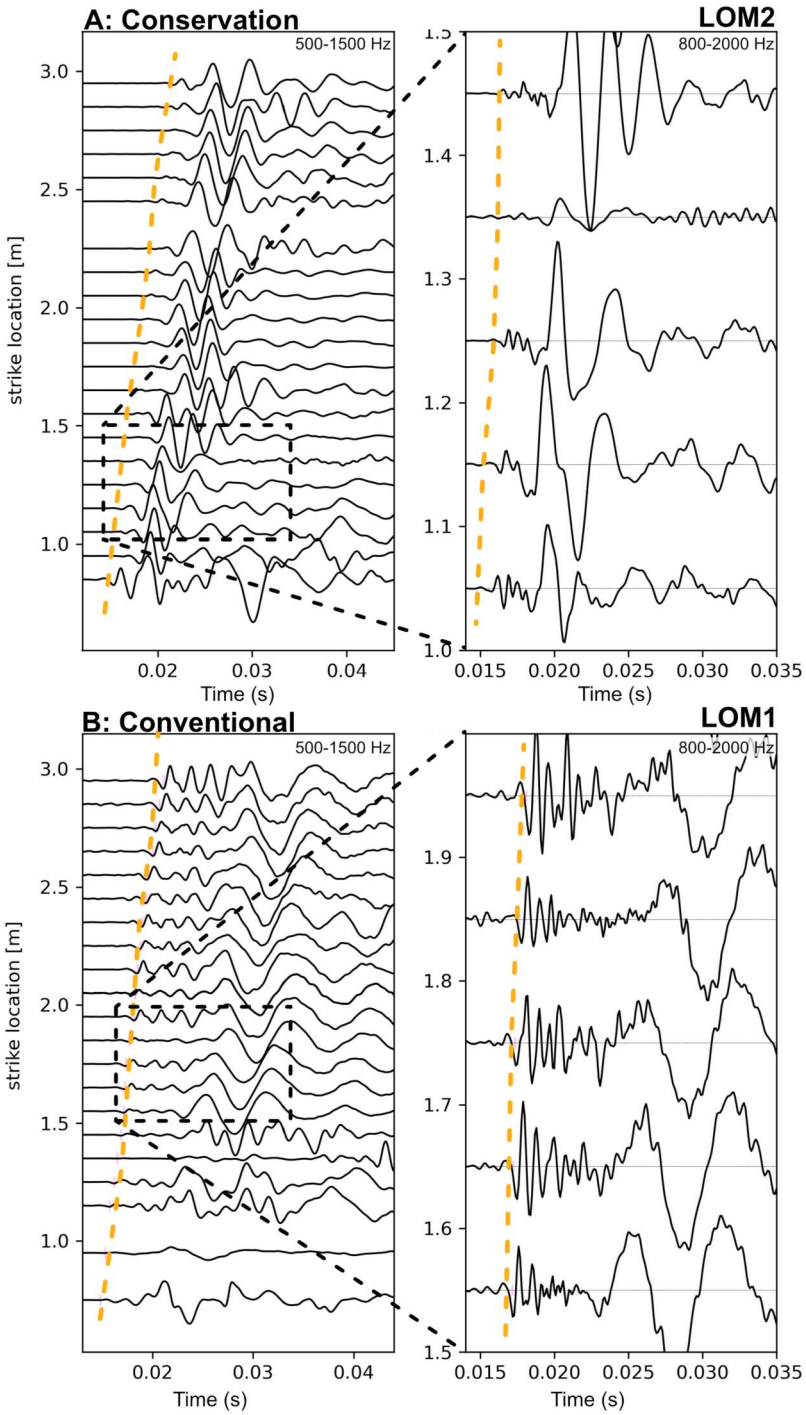

Figure 3. Common receiver gathers (i.e., recordings from multiple hammer strikes at the same geophone) in **A** the Conservation and **B** the Conventional treatments. Waveforms are plotted according to source location to highlight the move-out of seismic phases, and all traces are individually amplitude-normalized. The left panels provide an overview of all source distances, while the right panels zoom in on five selected distances. The orange dashed line marks the picked P-wave arrival times. Waveforms are bandpass filtered between 500–1500 Hz (left) and 800–2000 Hz (right), to enhance the visibility of the first arrival. The location of 'LOM1' (bottom) and 'LOM2' (top) in the experimental set-up is marked in figure 2(A).

We calculated data normality and homoscedasticity for the v_p model with the Shapiro Wilks Test and Bartlett's Test using the base `Rstats` package. The data was modelled using a generalised linear model using the `stats` package in `R` to determine the soil variable that are significant drivers of v_p. The model used dry bulk density as a fixed effect.

2.3. Bulk-density analysis of soil

One day after the seismic experiments, we used an excavator to extract 210 cores of soil beneath both seismic lines from $x = 5$ cm to $x = 295$ cm to a depth of $z = 50$ cm (figure 2(B)). Each core had a volume of 100 cm^3. The

horizontal spacing of the cores was 10 cm, the same as the spacing of the geophones. The samples were analysed for dry bulk density, volumetric moisture content, and stone mass (Methodologies are presented in Supplementary section 1).

We modelled the spatial correlation between the soil samples using variograms to estimate spatially distributed soil variables at upsampled locations. The models fitted to the variogram were automatically generated to compute the best fit using the `automap` package in `R` (Hiemstra *et al* 2009). We modelled bulk density using Matern semivariogram models for each treatment with varying values for the nugget, sill, and range, which were all automatically computed for the best fit (Conservation: $Nugget = 0.01$, $Sill = 0.03$, $Range = 26$, $\kappa = 10$. Conventional: $Nugget = 0.01$, $Sill = 0.03$, $Range = 33$, $\kappa = 0.6$). The semivariogram models and model statistics are presented in Supplementary figures 2 and 3. We used the variogram to perform Ordinary Kriging using `gstat`(Pebesma 2004) and checked the interpolation method of Ordinary Kriging for applicability using the Moran's I statistic for spatial autocorrelation using the `spdep` package in `R`(Bivand and Wong 2018). A k-nearest neighbours algorithm was applied to the extent coordinates to identify the spatial relationships among sampling locations and create a spatial weights matrix using a row-standardized (W) approach (Tiefelsdorf *et al* 1999). Using the spatial weights matrix, Moran's I test was conducted on the Kriging-predicted values to statistically assess the degree of spatial autocorrelation present in the predictions. The kriging models were cross validated using Leave-One-Out Cross-Validation (Kleijnen and Van Beers 2022), and indicated unbiased predictions (Conservation: $ME = 0.0005$, $RMSE = 0.118$, and $R^2 = 0.51$. Conventional: $ME = 0.0004$, $RMSE = 0.13$, and $R^2 = 0.36$).

3. Results

Wave propagation was different in the Conservation and Conventional treatments (figure 3). There was larger separation between the P-waves and later high-amplitude arrivals in the Conservation treatment. This suggests different Rayleigh wave characteristics in the topsoil and subsoil of the treatments, but we focus our analysis in this paper on the arrival time of the P-wave.

In seismic tomography, we assess the quality of a model using the chi-squared (χ^2) value, which quantifies how well the predicted data fit the observations relative to their assumed uncertainties, with values around 1 indicate a better fit. The final seismic models achieved reduced χ^2 of 0.927 for the Conservation treatment and χ^2 of 0.984 for the Conventional treatment, indicating a good fit to the observed data within the assigned uncertainty bounds (0.45–0.55 millisecond).

We found sharper contrast in the Conservation treatment which suggest denser, more cohesive top layers that are better resolved at ultra-high frequencies. The v_p ranged from approximately 300 m s^{-1} in the unconsolidated near-surface layers to about 600 m s^{-1} at around 40 cm depth. v_p was lowest near the surface with a mean velocity of 309.9 m s^{-1} ($SE = 1.72$) in the Conservation treatment and a mean of 293.1 m s^{-1} ($SE = 0.96$) in the Conventional treatment, and increases with depth in both treatments to 555.4 m s^{-1} ($SE = 6.39$) in the Conservation treatment and 429.8 m s^{-1} ($SE = 2.5$) in the Conventional treatment at 40 cm depth. Our analysis identified a significant increase in v_p ($\beta = 34.6$, $SE = 10.6$, $Z = 3.2$, $p = 0.002$) in the Conservation treatment compared to the Conventional treatment.

Our analysis of the soil samples using a linear mixed effects model indicates that the bulk density in the Conservation treatment is higher than in the Conventional treatment at all depths analysed (0–45 cm) ($\beta = -0.13$, $SE = 0.01$, $Z = -11.23$, $p < 0.0001$). The mean bulk density at 5 cm depth is 1.27 g cm^{-3} in the Conventional treatment and 1.36 g cm^{-3} in the Conservation treatment ($\beta = -0.09$, $SE = 0.03$, $Z = -3$, $p = 0.003$). At 45 cm depth, mean bulk density is 1.51 g cm^{-3} and 1.69 g cm^{-3} in the Conventional and Conservation treatments, respectively ($\beta = -0.17$, $SE = 0.03$, $Z = -5.5$, $p < 0.0001$). The increase of bulk density with depth was similar for both treatments (figures 4 and 5(A)).

Ordinary Kriging was applied to estimate bulk density across the experimental extent. The Moran's I analysis identified significant positive spatial autocorrelation ($MoransI = 6.29$, $p = < 0.0001$) in the data, indicating that soil bulk density is spatially clustered and not randomly distributed throughout the soil profile. This supports the use of spatial interpolation methods in this analysis. The spatial interpolation of soil bulk density for both experimental treatments is shown in figure 4.

The results of the seismic model were compared with interpolated bulk density measurements taken along the same transect (figure 5). In both datasets, a clear contrast between the two treatments is evident. The Conservation treatment shows generally higher bulk density and a more abrupt transition to denser layers.

In contrast, the Conventional treatment exhibits lower overall values and seismic velocities transition smoother and more gradual with depth. The patterns in v_p and bulk density were similar. Higher velocities were observed at 40 cm in the Conservation treatment than in the Conventional treatment. In line with the observations for the bulk densities, there was greater variation in velocities in the Conventional treatment, with a

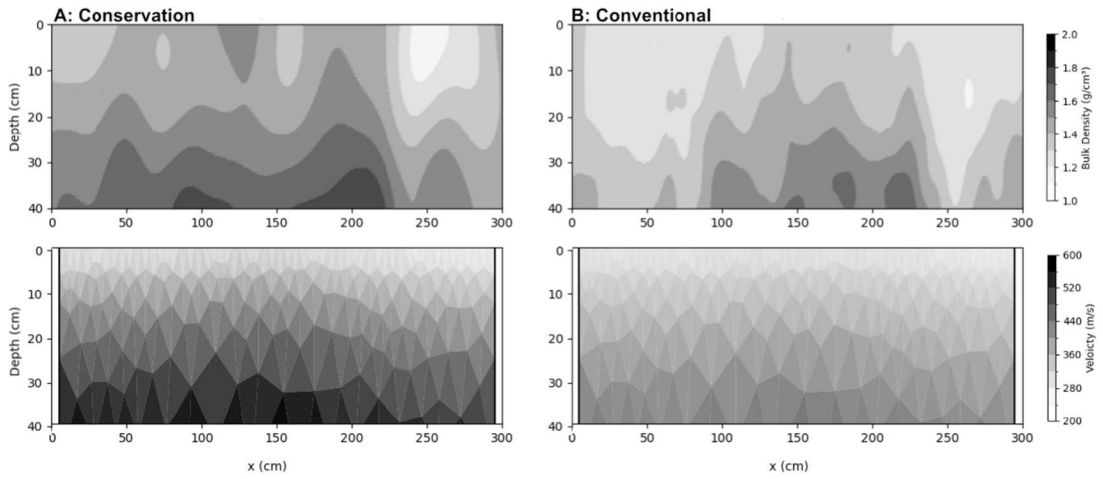

Figure 4. Comparison of bulk density and seismic imaging. The top panel shows interpolated bulk density across the transect of soil probes (see figure 2(B)) for both treatments: **A** Conservation left and **B** Conventional right. The bottom panel displays the corresponding seismic velocity models. Darker shades indicate higher bulk density and higher seismic velocities. Overall, the Conventional treatment shows lower values and a smooth transition from the top to the bottom. The Conservation treatment exhibits a more abrupt transition and higher values of bulk density and seismic velocity.

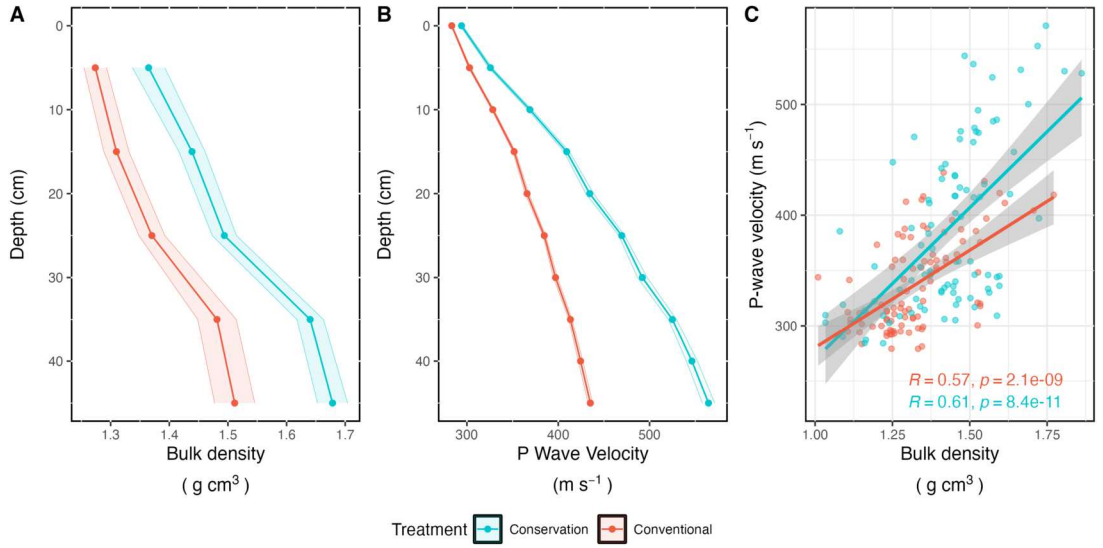

Figure 5. A: Soil bulk density (g cm^{-3}) $n = 30$ depth^{-1}. **B:** P-wave velocity (m s^{-1}). **C:** P-wave velocity and soil bulk density Pearson's correlation coefficient. Ribbon is equal to standard error of the mean. Each point represents a derived v_p value from the chosen depth grid and its corresponding bulk density measurement. V_p values are discretized samples of the continuous velocity field.

sharper transition of velocities evident. Pearson's correlation coefficient analysis identified a strong positive correlation between v_p and bulk density ($R = 0.57, p < 0.0001$) in the Conventional treatment and the Conservation treatment ($R = 0.61, p < 0.0001$). Statistical analysis identified bulk density as a highly significant driver of v_p ($\beta = 287, SE = 35, Z = 8.21, p < 0.001$).

4. Discussion

This study explores the use of ultra-high frequency seismology as a simple and scalable method for non-invasive soil structure assessment. By targeting decimetre-scale resolution using ultra-high frequency waves, we aim to quantify spatial variations in topsoil bulk density and examine their relationship to physical soil properties. Our results confirm that at ultra-high frequencies, seismic velocity correlates strongly with bulk density, confirming that ultra-high frequency seismic imaging can resolve subtle structural differences in soil profiles related to land management practices, supporting the use of seismic methods for rapid, non-invasive assessments of soil structure at the decimetre scale (Nissen-Meyer *et al* in prep., Jeffery *et al* in prep.).

The comparison between the two agricultural treatments reveals clear significant differences in soil bulk density as is commonly associated with different tillage systems (Soane *et al* 2012, Garbout *et al* 2013). In the Conservation treatment, we observe significantly higher bulk density, correlated with higher seismic compressional velocities, with a sharper and more clearly defined boundary in the seismic image.

This is in contrast to the Conventional treatment, where bulk density is significantly lower, seismic velocities are significantly lower, and the interface appears less distinct. This is the first instance in which ultra-high frequency seismic waves (>800 Hz) have been used in order to resolve soil physical characteristics at the approximately 10 cm scale of resolution.

Previous analysis of soil compaction using seismic waves have used lower frequencies and been constrained to a lower resolution of approximately 25 cm or above (Romero-Ruiz *et al* 2021, Carrera *et al* 2024). This scale of resolution can be insufficient for assisting with making agronomic decisions, such as whether a top soil is sufficiently compacted that remedial action is required.

Seismic P-wave velocities between 300-600 m s^{-1} compare well with previous studies (Carrera *et al* 2024). For the shallowest 10 cm, this requires frequencies of at least 1500, whereas at 40 cm depth a 10 cm-resolution is fully met by frequencies above 3000 Hz. This shows the need to push seismic methods well into the ultra-high frequency regime if one needs to resolve even finer structure in a fully spatially explicit manner. However, in the case of onset P-wave traveltimes, and the imaging methodology used here, the assumption of infinite-frequency traveltimes seems to hold, as long as the onset traveltimes are robustly pickable and stable with respect to the wider frequency spectrum (Nissen-Meyer *et al* in prep.). When frequencies are too low to resolve a structure and waveforms are used instead of onset travel times, the resulting seismic image will be a smeared approximation of the true structure.

These observations suggest that no-tillage agricultural practices have deeper and more compacted soil layers, which in turn enhance seismic wave velocities. This is due to the transition period that occurs when a field shifts from conventional tillage to no-tillage practices. Improvements in soil bulk density can require several years under no-tillage soil management (Blanco-Canqui and Ruis 2018). Soil compaction is a large and growing issue globally, driven by the increasing size of agricultural vehicles (Gürsoy 2021) and the increasing numbers of livestock (Zhang *et al* 2022). In England and Wales alone, the economic costs of compaction were estimated to be £472 million annually in 2015 (Graves *et al* 2015). It has been estimated that long-term productivity losses of 10–20% globally can be expected due to the interaction between soil compaction and water erosion (Sonderegger and Pfister 2021).

While porosity was not directly measured, it is inversely proportioned to bulk density (Robinson *et al* 2022). It is currently posited to have strong potential as an indicator of soil health due to the strong relationship with biological activity in its genesis, as well as the important role it plays in numerous soil functions such as facilitating water infiltration and root penetration as well as gas exchange (Neal *et al* 2020). However, there are currently no non-invasive means of quantifying porosity in the field. The approach outlined in this paper therefore shows strong potential for application as a further tool to help quantify soil health.

Another major advantage of this experimental set-up is that each hammer-source seismic experiment takes only about 10 seconds to conduct, and the full acquisition of a survey line typically takes between 1 to 2 hours. In contrast, the soil analysis involved digging 210 individual holes and performing time-consuming laboratory analyses for each sample. This highlights the practical value of the seismic method, not only in terms of resolution and spatial coverage but also in reducing the time, labour, and cost associated with soil characterization as discussed by Bloem *et al* (2025).

5. Conclusions

The application of ultra-high frequency seismic approaches shows strong potential for identifying soil compaction by quantifying changes in bulk density. As a spatially explicit and non-invasive method, it operates at a resolution that may be sufficient to support agronomic and land management decisions. Furthermore, it holds promise as an important predictor variable in future machine learning-based pedotransfer models for soil processes.

Our method offers a fast, non-invasive alternative to traditional sampling, capable of capturing high-resolution spatial variability of soil properties such as bulk density. By scaling this approach, we can help bridge the gap between coarse continental-scale models and the finer, field-level data needed for site-specific land management. In the long term, seismic-derived measurements could serve as an important input for machine learning models (Nissen-Meyer *et al* in prep.), enabling more localized and accurate predictions of soil properties—and ultimately supporting more informed, data-driven decisions in agronomy and land use.

With further refinement—such as inclusion of S-phases, full-waveform inversion, Bayesian inversion approaches, machine-learning automation, and lab analyses of soil texture, carbon, and organic matter—this

method could provide a powerful alternative to conventional, time-consuming soil sampling techniques. While the present study focuses on a single soil type and seasonal snapshot, further validation across different soil textures, moisture regimes, and climatic conditions will be essential to assess broader applicability. Our preliminary analysis of v_p-moisture relationships suggests a weaker correlation compared to bulk density, but seasonal and site-specific effects should be quantified in future multi-site experiments. Building on this, subsequent work will investigate S-wave velocities (vs) and explore additional soil parameters, such as porosity and moisture content, through targeted experiments and expanded analyses.

Acknowledgments

The authors would like to thank Shavington and Coverley Estate Management Ltd for providing access to the land used in this experiment. We are grateful to Martin and Bill Bower for their management of the agricultural field operations, and to Alistair Sibbett and Paul Cawood for overseeing the agronomy. We also thank the CERC staff at Harper Adams University for their support in processing soil samples. The agricultural experiment was funded by the Biotechnology and Biological Sciences Research Council (BBSRC) and BASE-UK. Earth Rover Program is support by the Bezos Earth Fund and the Read Foundation. Special Thanks go to Jo Howard and Deborah Harris from Earth Rover Program who supported all of the logistical operations.

Data accessibility and code usage

Seismic waveform processing was conducted using the Python package `ObsPy`, while phase picking was performed with `Pyrocko` ('Snuffler' package). Seismic imaging was carried out using `pyGIMLi`.

Statistical analysis and spatial interpolation were conducted in R. We used `lme4` to fit linear and generalized linear mixed-effects models, and `emmeans` for post-hoc analyses. Interpolation workflows made use of `automap` for automatically estimating interpolation variograms and `gstat` for variogram modeling and ordinary kriging. Autocorrelation testing was performed with `spdep`, and figures were created using `ggplot2` (Wickham 2016).

Declaration of competing interest

The authors declare no competing interests and that they have no known competing financial interests or personal relationships that could have appeared to influence the work reported in this paper.

Data availability statement

The data that support the findings of this study will be openly available following an embargo at the following URL/DOI: https://doi.org/10.5281/zenodo.15431293. Data will be available from 31 December 2025.

Author contributions

Maria Tsekhmistrenko 0000-0003-4315-6366
Data curation (equal), Formal analysis (equal), Visualization (equal), Writing – original draft (equal), Writing – review & editing (equal)

Joe Collins 0009-0009-8061-6166
Data curation (equal), Formal analysis (equal), Visualization (equal), Writing – original draft (equal), Writing – review & editing (equal)

Hugo Bloem 0000-0002-4205-0597
Data curation (equal), Formal analysis (equal), Writing – original draft (equal), Writing – review & editing (equal)

Tina Fallah 0000-0002-1123-1790
Data curation (equal), Formal analysis (equal), Writing – original draft (equal), Writing – review & editing (equal)

Jeroen Ritsema 0000-0003-4287-7639
Writing – original draft (equal), Writing – review & editing (equal)

Simon Jeffery 0000-0003-1014-9100
Conceptualization (equal), Funding acquisition (equal), Investigation (equal), Project administration (equal), Resources (equal), Writing – original draft (equal)

Tarje Nissen-Meyer 0000-0002-9051-1060
Conceptualization (equal), Investigation (equal), Project administration (equal), Resources (equal), Writing – original draft (equal), Writing – review & editing (equal)

References

Baker G, Steeples D and Schmeissner C 2002 The effect of seasonal soil-moisture conditions on near-surface seismic reflection data quality *First Break* **20** 35–41
Basset C, Abou Najm M, Ghezzehei T, Hao X and Daccache A 2023 How does soil structure affect water infiltration? a meta-data systematic review *Soil Tillage Res.* **226** 105577
Bivand R and Wong D W S 2018 Comparing implementations of global and local indicators of spatial association *Test* **27** 716–48
Blanco-Canqui H and Ruis S J 2018 No-tillage and soil physical environment *Geoderma* **326** 164–200
Bloem H, Ritsema J, Tsekhmistrenko M, Collins J, Jeffery S and Nissen-Meyer T 2025 Affordable seismic analysis of soil at the decimetre scale *Submitted to Seismica*
Carrera A, Barone I, Pavoni M, Boaga J, Dal Ferro N, Cassiani G and Morari F 2024 Assessment of different agricultural soil compaction levels using shallow seismic geophysical methods *Geoderma* **447** 116914
Chen S, Chen Z, Zhang X, Luo Z, Schillaci C, Arrouays D, Richer-de-Forges A C and Shi Z 2024 European topsoil bulk density and organic carbon stock database (0-20 cm) using machine-learning-based pedotransfer functions *Earth System Science Data* **16** 2367–83
Collins J 2025 A Systems-level Evaluation of Conservation Agriculture in the UK *Unpublished PhD thesis* Harper Adams University
Dexter A 1988 Advances in characterization of soil structure *Soil Tillage Res.* **11** 199–238
dos Santos W P, Vaz C M P, Martin-Neto L, Anselmi A, Tomasella J, de Souza Costa F, Albuquerque J A, de Jong van Lier Q, Galbieri R and Perina F J 2025 Predicting bulk density in Brazilian soils for carbon stocks calculation: a comparative study of multiple linear regression and Random Forest models using continuous and categorical variables *Discover Soil* **2** 7
El-Emam M M, Khan Z H, Mohammad O and Amer M 2019 Effect of water content, void ratio and clay content on sand p-wave velocity *Proceedings of the 4th World Congress on Civil, Structural, and Environmental Engineering (CSEE'19). Paper No. ICGRE* vol 175
Garbout A, Munkholm L J and Hansen S B 2013 Tillage effects on topsoil structural quality assessed using X-ray CT, soil cores and visual soil evaluation *Soil Tillage Res.* **128** 104–9
Graves A R, Morris J, Deeks L K, Rickson R J, Kibblewhite M G, Harris J A, Farewell T S and Truckle I 2015 The total costs of soil degradation in England and Wales *Ecol. Econ.* **119** 399–413
Gürsoy S 2021 Soil compaction due to increased machinery intensity in agricultural production: its main causes, effects and management *Technology in Agriculture* (IntechOpen) ch 5 (https://doi.org/10.5772/intechopen.98564)
Hallett S H, Sakrabani R, Keay C A and Hannam J A 2017 Developments in land information systems: examples demonstrating land resource management capabilities and options *Soil Use and Management* **33** 514–29
Hartemink A E, Zhang Y, Bockheim J G, Curi N, Silva S H G, Grauer-Gray J, Lowe D J and Krasilnikov P 2020 Chapter three - soil horizon variation: a review *Advances in Agronomy* vol 160 ed D L Sparks (Academic) pp 125–85
Heimann S *et al* (2017) Pyrocko-an open-source seismology toolbox and library. GFZ Data Services (https://doi.org/10.5880/GFZ.2.1.2017.001)
Hiemstra P H, Pebesma E J, Twenhöfel C J and Heuvelink G B 2009 Real-time automatic interpolation of ambient gamma dose rates from the Dutch radioactivity monitoring network *Comput. Geosci.* **35** 1711–21
Hollis J M, Hannam J and Bellamy P H 2012 Empirically-derived pedotransfer functions for predicting bulk density in European soils *Eur. J. Soil Sci.* **63** 96–109
Jarvis N, Coucheney E, Lewan E, Klöffel T, Meurer K H E, Keller T and Larsbo M 2024 Interactions between soil structure dynamics, hydrological processes, and organic matter cycling: A new soil-crop model *Eur. J. Soil Sci.* **75** e13455
Jeffery S, Collins J, Tsekhmistrenko M, Bloem H, Ritsema J and Nissen-Meyer T [manuscript in preparation] Soil Vibes - a case for high frequency seismology for subsurface soil exploration
Kleijnen J P and Van Beers W C 2022 Statistical tests for cross-validation of kriging models *INFORMS Journal on Computing* **34** 607–21
Lehmann J, Bossio D A, Kögel-Knabner I and Rillig M C 2020 The concept and future prospects of soil health *Nat. Rev. Earth Environ.* **1** 544–53
Liu S, Wei Y, Post W M, Cook R B, Schaefer K and Thornton M M 2013 The Unified North American Soil Map and its implication on the soil organic carbon stock in North America *Biogeosciences* **10** 2915–30
Lu Z, Wilson G V and Shankle M W 2019 Measurements of soil profiles in the vadose zone using the high-frequency surface waves method *J. Appl. Geophys.* **169** 142–53
Minasny B, McBratney A B, Malone B P and Wheeler I 2013 Chapter one - digital mapping of soil carbon *Advances in Agronomy* vol 118 ed D L Sparks (Academic) pp 1–47
Neal A L, Bacq-Labreuil A, Zhang X, Clark I M, Coleman K, Mooney S J, Ritz K and Crawford J W 2020 Soil as an extended composite phenotype of the microbial metagenome *Sci. Rep.* **10** 10649
Nissen-Meyer T, Tsekhmistrenko M, Bloem H, Collins J, Ritsema J and Jeffery S [manuscript in preperation] Soilsmology: revealing soil health by non-destructive, scalable seismic monitoring
Nolet G 2008 A breviary of seismic tomography *A Breviary of Seismic Tomography* vol 324 (Cambridge Press)
Nyéki A, Daróczy B, Kerepesi C, Neményi M and Kovács A J 2022 Spatial variability of soil properties and its effect on maize yields within field—A case study in hungary *Agronomy* **12** 395
Orgiazzi A, Ballabio C, Panagos P, Jones A and Fernández-Ugalde O 2018 LUCAS Soil, the largest expandable soil dataset for Europe: a review *Eur. J. Soil Sci.* **69** 140–53

Park J and Kim J 2023 Role of temperature-dependent interfacial tension on shear wave velocity for energy geosystems *Sensors* **23** 8709
Pebesma E J 2004 Multivariable geostatistics in S: the gstat package *Comput. Geosci.* **30** 683–91
Pimentel D 2006 Soil erosion: a food and environmental threat *Environment, Development and Sustainability* **8** 119–37
Rawlinson N, Pozgay S and Fishwick S 2010 Seismic tomography: a window into deep earth *Phys. Earth Planet. Inter.* **178** 101–35
Robinson D, Thomas A, Reinsch S, Lebron I, Feeney C, Maskell L, Wood C, Seaton F, Emmett B and Cosby B 2022 Analytical modelling of soil porosity and bulk density across the soil organic matter and land-use continuum *Sci. Rep.* **12** 7085
Romero-Ruiz A, Linde N, Baron L, Solazzi S G, Keller T and Or D 2021 Seismic signatures reveal persistence of soil compaction *Vadose Zone J.* **20** e20140
Rücker C, Günther T and Wagner F M 2017 pyGIMLi: an open-source library for modelling and inversion in geophysics *Computers and Geosciences* **109** 106–23
Saxton K E, Rawls W J, Romberger J S and Papendick R I 1986 Estimating generalized soil-water characteristics from texture *Soil Sci. Soc. Am. J.* **50** 1031–6
Scholes R *et al* 2018 Summary for policymakers of the assessment report on land degradation and restoration of the Intergovernmental Science- Policy Platform on Biodiversity and Ecosystem Services *Intergovernmental Science-Policy Platform on Biodiversity and Ecosystem Services (IPBES)* 1–44
Sharma D K, Tomar S and Chakraborty D 2017 Role of earthworm in improving soil structure and functioning *Curr. Sci.* **113** 1064–71
Soane B D, Ball B C, Arvidsson J, Basch G, Moreno F and Roger-Estrade J 2012 No-till in northern, western and south-western Europe: a review of problems and opportunities for crop production and the environment *Soil Tillage Res.* **118** 66–87
Sonderegger T and Pfister S 2021 Global assessment of agricultural productivity losses from soil compaction and water erosion *Environ. Sci. Technol.* **55** 12162–71
Suuster E, Ritz C, Roostalu H, Reintam E, Kõlli R and Astover A 2011 Soil bulk density pedotransfer functions of the humus horizon in arable soils *Geoderma* **163** 74–82
Tiefelsdorf M, Griffith D and Boots B 1999 A variance-stabilizing coding scheme for spatial link matrices *Environment and Planning A* **31** 165–80
Tisdall J M and Oades J M 1982 Organic matter and water-stable aggregates in soils *J. Soil Sci.* **33** 141–63
Usowicz B and Lipiec J 2017 Spatial variability of soil properties and cereal yield in a cultivated field on sandy soil *Soil Tillage Res.* **174** 241–50
Wang Y 2012 Gauss-Newton method *WIREs Computational Statistics* **4** 415–20
Wickham H 2016 *Ggplot2: Elegant Graphics for Data Analysis* (Springer) (https://doi.org/10.1080/15366367.2019.1565254)
Zhang L *et al* 2022 A 130-year global inventory of methane emissions from livestock: trends, patterns, and drivers *Global Change Biol.* **28** 5142–58